The Measurement of Displacement with the Use of MEMS Sensors: Accelerometer, Gyroscope and Magnetometer

Article · June 2017

DOI: 10.14313/JAMRIS_2-2017/15

CITATIONS
0

READS
1,305

4 authors:

Agnieszka Kobierska
Lodz University of Technology
11 PUBLICATIONS **20** CITATIONS
SEE PROFILE

Leszek. Podsędkowski
Lodz University of Technology
46 PUBLICATIONS **238** CITATIONS
SEE PROFILE

Pawel Andrzej Poryzala
Lodz University of Technology
23 PUBLICATIONS **126** CITATIONS
SEE PROFILE

Piotr Rakowski
Lodz University of Technology
4 PUBLICATIONS **2** CITATIONS
SEE PROFILE

The measurement of Displacement with the Use of MEMS Sensors: Accelerometer, Gyroscope and Magnetometer

Submitted: 2nd January 2017; accepted: 14th April 2017

Agnieszka Kobierska, Leszek Podsędkowski, Paweł Poryzała, Piotr Rakowski

DOI: 10.14313/JAMRIS_2-2017/15

Abstract:
The paper presents the method of determining the global orientation of links of the measuring arm by gauging the angles of the links relative to the vector of the gravitational and magnetic field using inertial sensors. A method of using Kalman filter to average the results is presented as a test on two-links measuring arm equipped with accelerometers and magnetometers placed on each of the links and analysis of measurement results in terms of repeatability. There was demonstrated the ability of creating kinematic chain. Instead of determining the position of the final link on the basis of the measurement of angles in relation to the previous links from the end to the base of the arm, it is possible to define links global orientation by measuring angles of links in reference to the vectors of the gravity field and the magnetic field, in global coordinate system.

Keywords: *Kalman filter, MEMS sensors, measuring arm*

1. Introduction

Determination of kinematic chain last point's location based on location of each link constitutes an issue in which usage of precise encoders (optical or magnetic) is common in measuring angle of joint's rotation. This solution is expensive, however it provides high accuracy of results obtained. Specified, mutual location of individual links in each direction is not dependent from the attachment position of encoders because they directly indicate angular position of rotary axis of exact degree of freedom. They are not used in solutions as this in case of small size devices. The research on solution to miniaturise measuring arm in limited workspace began with the measurement with usage of inertial sensors [1]. However, all of the inertial measuring systems are exposed to integration errors: small acceleration and velocity measurement errors are being integrated in increasingly large velocity errors which magnify themselves to even more significant position errors [3], [2], [1]. New position is calculated based on previous calculated location, measured acceleration and angular velocity. Those errors cumulate approximately proportional to time, because the primary position constitute an input value. For that reason, the position must be periodically adjusted to another additional type of navigation system.

However it is possible to create kinematic chain, which eliminates determining position of the last link, based on measurements of angles related to previous links from the end to the base, Instead, it is possible to determine the global orientation by measuring angles of links in respect to the vectors of the gravity field and the magnetic field, which are in global coordinate system.

The paper presents measuring method with a simple two-links measuring arm, equipped with accelerometers and magnetometers placed on each of the links and analysis of measurement results in terms of repeatability. In chapter II, the analysis of kinematic structure and method of using Kalman filter to average the results will be presented, in chapter III research stand and in chapter IV measurements results will be presented and whole will be summed up in chapter V.

2. Theory

2.1. Kinematic Structure

Unequivocal definition of position of the link its initial point requires defining its orientation in basic coordinate system which is connected to an immovable base. To describe kinematic structure of measuring arm (Fig. 1) the following parameters has been used: X_1,Y_1,Z_1 – global coordinate system located on link 1, X_2,Y_2,Z_2 – coordinate system attached to link 2, X_3,Y_3,Z_3 – coordinate system attached to link 3.

Vector $L=[L_X,L_Y,L_Z]$ has been specified by combining joints I and III and following angles: θ_2 between L vector and X_2 – axis vector, θ_3 between L vector and X_3 vector, θ_Z between L vector and X_1Y_1 plane, θ_Y between X_1 – axis vector and L vector measured in X_1Y_1 plane,

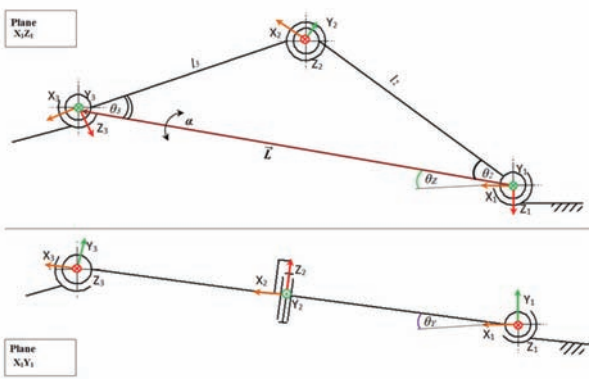

Fig. 1 Measuring arm's kinematic chain – plane X_1Z_1 and X_1Y_1

α as rotation of the plane defined by initial points of joints around L vector.

Links location is determined by L vector defined as:

$$\vec{L} = R_G^2 * [l_2\ 0\ 0]^T + R_G^3 * [l_3\ 0\ 0]^T, \quad (1)$$

where: R_G^2 – matrix of X_2,Y_2,Z_2 coordinate system rotation - connected with link 2,

$$R_G^2 = R_{\theta_Z} R_{\theta_Y} R_\alpha R_{\theta_2}, \quad (2)$$

R_G^3 – matrix of X_3,Y_3,Z_3 coordinate system rotation – connected with link 3,

$$R_G^3 = R_{\theta_Z} R_{\theta_Y} R_\alpha R_{\theta_3}, \quad (3)$$

R_α – rotation around X axis by α angle

$$R_\alpha = \begin{bmatrix} 1 & 0 & 0 \\ 0 & \cos\alpha & -\sin\alpha \\ 0 & \sin\alpha & \cos\alpha \end{bmatrix}, \quad (4)$$

$R_{\theta z}$ – rotation around Z axis by θ_Z angle

$$R_{\theta_z} = \begin{bmatrix} \cos\theta_z & -\sin\theta_z & 0 \\ \sin\theta_z & \cos\theta_z & 0 \\ 0 & 0 & 1 \end{bmatrix}, \quad (5)$$

$R_{\theta Y}$ – rotation around Y axis by θ_Y angle

$$R_{\theta_Y} = \begin{bmatrix} \cos\theta_Y & 0 & -\sin\theta_Y \\ 0 & 1 & 0 \\ \sin\theta_Y & 0 & \cos\theta_Y \end{bmatrix}, \quad (6)$$

$R_{\theta 2}$ – rotation around Y axis by θ_2 angle

$$R_{\theta_2} = \begin{bmatrix} \cos\theta_2 & 0 & -\sin\theta_2 \\ 0 & 1 & 0 \\ \sin\theta_2 & 0 & \cos\theta_2 \end{bmatrix}, \quad (7)$$

$R_{\theta 3}$ – rotation around Y axis by $(-\theta_3)$ angle

$$R_{\theta_3} = \begin{bmatrix} \cos\theta_3 & 0 & \sin\theta_3 \\ 0 & 1 & 0 \\ -\sin\theta_3 & 0 & \cos\theta_3 \end{bmatrix}. \quad (8)$$

Basing on the law of cosines we set:

$$cos\theta_3 = \frac{-l_2^2 + l_3^2 + \bar{L}^2}{2 l_3 \bar{L}} \quad (9)$$

$$cos\theta_2 = \frac{l_2^2 - l_3^2 + \bar{L}^2}{2 l_2 \bar{L}} \quad (10)$$

$$\sin\theta_2 = \frac{l_3}{l_2} sin\theta_3 \quad (11)$$

and

$$cos\theta_Z = \frac{L_X}{\sqrt{{L_x}^2 + {L_y}^2}} \quad (12)$$

$$cos\theta_Y = \frac{L_Z}{\sqrt{\bar{L}^2}} \quad (13)$$

In cylindrical coordinate system **L** vector: $\boldsymbol{Z} = L_z$;

$$\mathbf{R} = \sqrt{(L_x + L_y)}; \boldsymbol{\theta} = \text{atan2}(L_y, L_x).$$

If vector of the gravity G equal to:

$$G = \begin{bmatrix} 0 \\ 0 \\ G_z \end{bmatrix} \quad (14)$$

and vector of the magnetic field M, with the base of the measuring arm oriented towards Earth's magnetic pole:

$$M = \begin{bmatrix} 0 \\ m_y \\ m_z \end{bmatrix} \quad (15)$$

values of gravitational acceleration and magnetic field measured by sensor attached to 2 link equals:

$$a_2 = \begin{bmatrix} a_{x2}\ a_{y2}\ a_{z2} \end{bmatrix} = (R_G^2)^T * G, \quad (16)$$

$$m_2 = \begin{bmatrix} m_{x2}\ m_{y2}\ m_{z2} \end{bmatrix} = (R_G^2)^T * M, \quad (17)$$

And for 3 link we receive:

$$a_3 = \begin{bmatrix} a_{x3}\ a_{y3}\ a_{z3} \end{bmatrix} = (R_G^3)^T * G \quad (18)$$

$$m_3 = \begin{bmatrix} m_{x3} m_{y3} m_{z3} \end{bmatrix} = (R_G^3)^T * M \quad (19)$$

Based on equations (1–19) and selected data read by sensors direct dependence of **L** vector can be received. It can be seen that there is more available data than required to perform calculations and hence this redundancy can be used to increase accuracy of measurement. Despite the fact that the data read by sensors are highly noised, it is possible to use the following measurements as a static measurement because the arm does not perform dynamic movements. However it should be remembered that each sensor has different accuracy described as the noise of measurement covariance matrix and his uniqueness should be included while gauging the real location of arm. The references to Kalman filtration can be seen in bibliography [5–8]. It includes all of foregoing factors and sets the estimate of the state vector having the smallest covariance error.

2.2. Usage of the Extended Kalman Filter to Average the State Vector

While constructing Kalman filter, the state vector X, the output vector Z, the control vector U, discrete equation of state, the output equation, covariance matrix Q the noise of the process w_Q, covariance matrix R the noise of measurement w_R, the initial state X_0 and error covariance matrix of its estimation P_0 should be defined as follows:

The state vector X of the system:

$$X = \begin{bmatrix} L_x\ L_y\ L_z\ \alpha \end{bmatrix}^T \quad (20)$$

The output vector Z of the system:

$$Z = \begin{bmatrix} a_2 \\ m_2 \\ a_3 \\ m_3 \end{bmatrix} = \begin{bmatrix} a_{x2} \\ a_{y2} \\ a_{z2} \\ m_{x2} \\ m_{y2} \\ m_{z2} \\ a_{x3} \\ a_{y3} \\ a_{z3} \\ m_{x3} \\ m_{y3} \\ m_{z3} \end{bmatrix} \quad (21)$$

The control vector of the system is assumed as a rate of change of the α angle:

$$U=[0,0,0,\dot{\alpha}\Delta t] \quad (22)$$

determined on the base of gyroscope sensors attached to both links. From the methodological point of view more accurate would be to join this velocity to vector of state and values of measurements to vector of measurement. However, proposed solution is less demanding for computing reasons and due to consideration of gyroscope's measurement uncertainty, the noise of the process covariance matrix gives almost the same results.

For variables defined this way, the equation of state is defined as:

$$X_{k+1} = f(X_k, U_k) + w_Q = X_k + U_k + w_Q \quad (23)$$

and the measurement equation is defined as:

$$Z_k = h(X_k) + w_R \quad (24)$$

where relation h(X) combining direction of the gravity and the magnetic field read by sensors with variable of the state is non-linear and defined on the base of (1–19) equations. Due to the fact that measurement is assumed to be static where L vector remains constant and where change of α angle is unknown and rotated manually, the noise covariance matrices Q_{4x4} was assumed as zeros except (4,4) element, where substituted cubed standard deviation of radial velocity measurement. The noise of the measurement covariance matrix R_{12x12} has been defined as diagonal matrix with cubed standard deviation of individual sensors on the main diagonal of the matrix.

In this system we use equations of Kalman filter in **stage of prediction** – the prediction of the state at the timestep *k* based on the state estimate and control from previous timestep:

$$\widehat{\boldsymbol{X}}_{\boldsymbol{k|k-1}} = \boldsymbol{f}(\widehat{\boldsymbol{X}}_{\boldsymbol{k-1|k-1}}, \boldsymbol{U}_{\boldsymbol{k-1}}) \quad (25)$$

$$\boldsymbol{P}_{\boldsymbol{k|k-1}} = \boldsymbol{F}_{\boldsymbol{k-1}}\boldsymbol{P}_{\boldsymbol{k-1|k-1}}\boldsymbol{F}_{\boldsymbol{k-1}}^{\boldsymbol{T}} + \boldsymbol{Q}_{\boldsymbol{k-1}} \quad (26)$$

in **stage of filtering** – the updating of the state estimator and error covariance matrix of the state based on the measurement inputs at the timestep:

$$\widehat{\boldsymbol{Y}}_{\boldsymbol{k}} = \boldsymbol{Z}_k - h(\widehat{\boldsymbol{X}}_{k|k-1}) \quad (27)$$

$$\boldsymbol{S}_k = \boldsymbol{H}_k\boldsymbol{P}_{\boldsymbol{k|k-1}}\boldsymbol{H}_k^{\boldsymbol{T}} - \boldsymbol{R}_k \quad (28)$$

$$\boldsymbol{K}_k = \boldsymbol{P}_{\boldsymbol{k|k-1}}\boldsymbol{H}_k^{\boldsymbol{T}}\boldsymbol{S}_k^{-\boldsymbol{1}} \quad (29)$$

$$\widehat{\boldsymbol{X}}_{\boldsymbol{k|k}} = \widehat{\boldsymbol{X}}_{\boldsymbol{k|k-1}} + \boldsymbol{K}_k\widehat{\boldsymbol{Y}}_{\boldsymbol{k}} \quad (30)$$

$$\boldsymbol{P}_{\boldsymbol{k|k}} = (\boldsymbol{I} - \boldsymbol{K}_k\boldsymbol{H}_k)\boldsymbol{P}_{\boldsymbol{k|k-1}} \quad (31)$$

where:

$$\boldsymbol{F}_{\boldsymbol{k-1}} = \frac{\boldsymbol{\partial f}}{\boldsymbol{\partial x}}\Big|_{\widehat{\boldsymbol{x}}_{\boldsymbol{k-1|k-1}}, \boldsymbol{u}_{\boldsymbol{k-1}}} = \boldsymbol{I}_{\boldsymbol{4x4}} \quad (32)$$

$\boldsymbol{F}_{\boldsymbol{k\text{-}1}}$ is the state transition model which is applied to the previous state x_{k-1},

$$\boldsymbol{H}_{\boldsymbol{k}} = \frac{\boldsymbol{\partial h}}{\boldsymbol{\partial x}}\Big|_{\widehat{\boldsymbol{x}}_{\boldsymbol{k|k-1}}} = \left[\frac{\boldsymbol{\partial Z}}{\boldsymbol{\partial \theta_3}}, \frac{\boldsymbol{\partial Z}}{\boldsymbol{\partial \theta_y}}, \frac{\boldsymbol{\partial Z}}{\boldsymbol{\partial \theta_z}}, \frac{\boldsymbol{\partial Z}}{\boldsymbol{\partial \alpha}}\right]_{\boldsymbol{12x4}}; \quad (33)$$

$\boldsymbol{H}_{\boldsymbol{k}}$ is the observation model which maps the true state space into the observed space. For example (34):

$$\frac{\boldsymbol{\partial Z}}{\boldsymbol{\partial \alpha}} =$$

$$\left[\frac{-\mathrm{G_z l_3}\sin\alpha\cos\theta_y\sin\theta_3}{\mathrm{l_2}},\right.$$

$$\mathrm{G_z}\cos\alpha\ \cos\theta_y,$$

$$-\mathrm{G_z}\sin\alpha\ \cos\theta_y\left(\sqrt{\frac{\mathrm{l_3}^2\sin(\theta_3)^2}{\mathrm{l_2}^2}+\mathbf{1}}\right),$$

$$\frac{-(\mathrm{l_3}\sin\theta_3(m_y\cos\alpha\cos\theta_z+m_z\sin\alpha\cos\theta_y-m_y\sin\alpha\sin\theta_y\sin\theta_z)}{\mathrm{l_2}},$$

$$m_z\cos\alpha\cos\theta_y - m_y(\sin\alpha\cos\theta_z + \cos\alpha\sin\theta_y\sin\theta_z),$$

$$-\left(\sqrt{\frac{\mathrm{l_3}^2(\cos(\theta_3)^2-1)}{\mathrm{l_2}^2}+1}\right)(m_y\cos\alpha\cos\theta_z +$$

$$m_z\sin\alpha\cos\theta_y - m_y\sin\alpha\sin\theta_y\sin\theta_z),$$

$$\mathrm{G_z}\sin\alpha\cos\theta_y\sin\theta_3,$$

$$\mathrm{G_z}\cos\alpha\cos\theta_y,$$

$$-\mathrm{G_z}\sin\alpha\cos\theta_3\cos\theta_y,$$

$$\sin\theta_3\,(m_y\cos\alpha\cos\theta_z + m_z\sin\alpha\cos\theta_y -$$

$$m_y\sin\alpha\sin\theta_y\sin\theta_z),$$

$$m_z\cos\alpha\cos\theta_y - m_y(\sin\alpha\cos\theta_z +$$
$$\cos\alpha\sin\theta_y\sin\theta_z),$$

$$-m_y\cos\theta_3\left(\cos\alpha\cos\theta_z - \sin\alpha\sin\theta_y\sin\theta_z\right) -$$

$$\left.m_z\sin\alpha\cos\theta_y\sin\theta_3\right]_{12x1}. \quad (34)$$

2.4. Research

To conduct the tests, the research stand (Fig. 2) mechanism has been assembled using four links: (1, 2, 3, 4) connected with two joints (no. I, III) of 3DoF and joint (no. II) of 1DoF. Individual links have been manufactured as 3D prints of VeroClear material. On each link, the sensor AltIMU 10 (5) has been placed, containing three-axis accelerometer (scale range ±2 g, resolution 0.06 mg/LSB), three-axis magnetometer (scale range ±2 gauss, resolution 0.06 mgauss/LSB) and three-axis gyroscope (scale range ±245 dps, resolution 0.004 dps/LSB) [9].

There can be seen that discussed measuring arm with fixed first and last joint has an additional degree of freedom: rotation of arm around axis between both spherical joints. During tests, two methodologies were used: measuring arm was fixed or was forced to perform slow oscillations around axis between both spherical joints.

From many conducted tests of the arm, in this paper the following ones were described:

1. Measurement of base position „0": 5 measurements with and without oscillations around α angle.

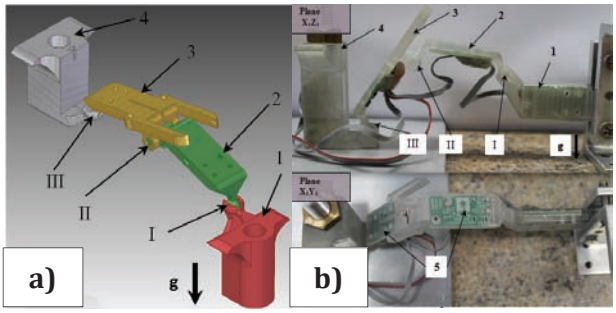

Fig. 2. Measuring arm model – a) CAD model and, b) 3D printed model

2. Measurement of displacement in **X** direction, by 2.0 mm in range to 10 mm from position „0": 5 measurements with and without oscillations around α angle.
3. Measurement of displacement in **Z** direction, by 3.2 mm in range to 16.0 mm from position „0": 5 measurements with and without oscillations around α angle.

Table1. The base position measurement's accuracy

The base position „0"		Ref. meas. [mm]	Middle meas. [mm]	Δ [mm]	δ [%]	σ [mm]
without osc.	**|L|** [mm]	61.82	61.44	±0.57	0.9	0.23
	R [mm]	57.06	56.54	±0.79	1.4	0.12
	θ [rad]	1.58	1.19	±0.42	26.7	0.06
	Z [mm]	-23.79	-24,04	±0.56	2.4	0.12
with osc.	**|L|** [mm]	61.82	61.61	±0.28	0.4	0.23
	R[mm]	57.06	56.76	±0.40	2.7	0.13
	θ [rad]	1.58	1.12	±0.48	28	0.01
	Z [mm]	-23.79	-23.97	±0.35	2	0.16

Table 2. Accuracy of displacement's measurement along Z axis

Displacem. along **Z** axis [mm]		Ref. meas. [mm]	Middle meas. [mm]	Δ [mm]	δ [%]	σ [mm]
without osc.	-3.11	-3.11	-2.88	±0.36	2.39	0.08
	-6.24	-6.24	-5.95	±0.33	2.18	0.03
	-9.34	-9.34	-9.28	±0.10	0.67	0.03
	-12.51	-12.51	-12.18	±0.41	2.77	0.08
	-15.65	-15.65	-15.70	±0.08	0.53	0.02
with osc.	-3.11	-3.11	-3.07	±0.08	0.6	0.04
	-6.24	-6.24	-6.14	±0.25	1.7	0.14
	-9.34	-9.34	-9.28	±0.14	0.9	0.08
	-12.51	-12.51	-12.38	±0.24	1.6	0.07
	-15.65	-15.65	-15.71	±0.12	0.8	0.06

Before attempting to accomplish measurements, the calibration of sensors has been performed to define indication values of individual vector's components in respect to the gravity field and the magnetic field of the Earth. Data from sensors have been read for 20 s with sampling frequency equal to 100 Hz, which allow to receive 2000 samples. Reference measurement has been performed with the usage of digital caliper with accuracy of 0.01 mm. Definition of length of links (l_2) and (l_3) has been based on the CAD model.

2.4. Results

Using Matlab software, functions, describing each data presented in section 2, have been created. During tests, huge variety of results connected with arm rotation around vertical axis has been noticed. According to that fact, the results were presented in cylindrical coordinate system as presented:

$$\boldsymbol{Z}=L_z;\ \mathbf{R}=\sqrt{\left(L_x+L_y\right)};\ \boldsymbol{\theta}=\operatorname{atan2}(L_y,L_x).$$

It can be seen that value of error is slightly smaller for the measurements with oscillations than for the case without oscillations, however the differences are not significant.

Due to the high value of absolute error of measurement **θ** angle (Δ=±0,42 rad). Following measurements has been focused on determining accuracy of measuring **Z** and **R** parameters. Results of measurements described in Table 2 show increased accuracy of measurements in model with applied oscillations of measuring arm's links around α. At the same time there can be seen increase of accuracy of displacement measurement in relation to displacement measurements described in Table 1. Similar results presented in table 3 were achieved for change of location in r direction.

During the measurements, magnetic sensor's measurement has the biggest influence on changes of displacement in θ direction. For example it can be disrupted by ferromagnetic materials or devices containing magnets like mobile phone. On the other hand, accuracy of position for measurements in the radial and vertical direction does not exceed ± 0.5 mm. Relative error of displacement measurements has been appointed as relation between maximal absolute error and range of displacement which is 10 mm. Very small value of standard deviation of measurements is worth to be noticed. It may indicate that prevailing cause of error is constituted by reference measurement, yet only future research can confirm this hypothesis.

3. Summary

Simple research stand has been set as basic two-link measuring arm. Global orientation of its links has been defined by measuring angles of joints in relation to vectors of the gravitational and magnetic field in global coordinate system. The paper presents the method of measurement with usage of the measuring arm equipped with accelerometers and magnetometers placed on each of the measuring arm links. Also there is presented analysis of system's kinematics and method of using Kalman filter to average the results. Analysis of measurements, in terms of repeatability, shows measurement's accuracy on level of ±0.5 mm along **Z** and **R** direction was described.

The results obtained from the magnetometer are strongly affected by external magnetic fields. The optained accuracy in the radial and vertical direction

Table 3. Accuracy of displacement's measurement along R axis

Displacem. along **R** axis [mm]		Ref. meas. [mm]	Middle meas. [mm]	Δ [mm]	δ [%]	σ [mm]
Without osc.	-2	-1.99	-1.77	±0.25	2.5	0.01
	-4	-3.90	-3.45	±0.45	4.5	0.02
	-6	-5.72	-5.75	±0.04	0.4	0.01
	-8	-7.45	-7.35	±0.10	1.0	0.02
	-10	-9.07	-9.22	±0.16	1.6	0.01
with osc.	-2	-1.99	-1.76	0.32	3.2	0.07
	-4	-3.90	-3.44	±0.47	4.7	0.02
	-6	-5.72	-5.63	±0.14	1.4	0.03
	-8	-7.45	-7.21	±0.24	2.4	0.01
	-10	-9.07	-9.13	±0.08	0.8	0.02

was the result of a high repeatability and accuracy of accelerometers. These conclusions were an impulse to seek another, limited cost, method of measurement, which would allow to get a high accuracy not only in two but in all six degrees of freedom.

It is possible to determine the joint angle based on data from the accelerometer placed on two links combined with rotary joint. It's rotation axis should always be inclined from the vertical direction. For a plurality of such links connected in series of the pivot joints and with triaxial accelerometer placed on each of links, we can get a measurement of the bending angle of each of the joints. Of course, as in the previous case the rotation axis of joints should be inclined from the vertical direction.

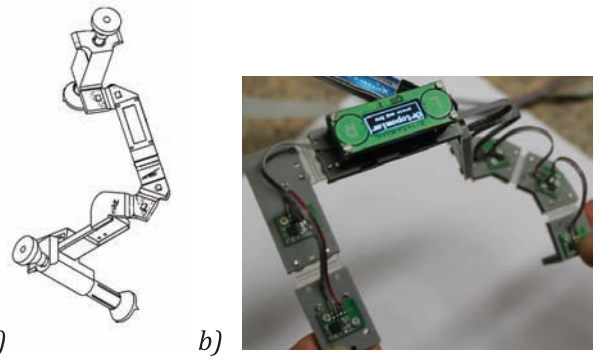

a) *b)*

Fig. 3. 6D arm a) CAD model; b) 3D printed model

In such a case it is possible to create kinematic chain with six degrees of freedom, measuring both the orientation and the position of the end effector in a coordinate system associated with the initial link. Fig. 3 presents a CAD model and 3D printing views of such arm. The arm consists of seven links connected with six rotary joints. In following research measuring algorithm will be developed along with the studies on the accuracy of arm with six degrees of freedom.

AUTHORS

Agnieszka Kobierska – Lodz University of Technology, Institute of Machine Tools and Production Engineering, 1/15 B. Stefanowskiego Street, 90-924 Lodz, Poland. E-mail: agnieszka.kobierska@p.lodz.pl.

Leszek Podsędkowski* – Lodz University of Technology, Institute of Machine Tools and Production Engineering, 1/15 B. Stefanowskiego Street, 90-924 Lodz, leszek.podsedkowski@p.lodz.pl

Paweł Poryzała – Lodz University of Technology, Institute of Electronics , 211/215 Wolczanska Street, 90-924 Lodz, pawel.poryzala@p.lodz.pl

Piotr Rakowski – Lodz University of Technology, Institute of Machine Tools and Production Engineering, 1/15 B. Stefanowskiego Street, 90-924 Lodz, piotr.rakowski@edu.p.lodz.pl

*Corresponding author

REFERENCES

[1] P. Cheng, B. Oelmann, "Joint-Angle Measurement Using Accelerometers and Gyroscopes—A Survey", *IEEE Transactions On Instrumentation And Measurement* vol. 59, no. 2, 2010, 404–414. DOI: 10.1109/TIM.2009.2024367.

[2] M. El-Gohary, J. McNames, "Human Joint Angle Estimation with Inertial Sensors and Validation with A Robot Arm", *IEEE Transactions On Biomedical Engineering*, vol. 62, no. 7, 2015, 1759–1767. DOI: 10.1109/TBME.2015.2403368.

[3] M. Quigley et al., "Low-cost Accelerometers for Robotic Manipulator Perception". In: *2010 IEEE/RSJ International Conference on Intelligent Robots and Systems*, October 18–22, 2010, 6168–6174. DOI: 10.1109/IROS.2010.5649804.

[4] Y. Wang, B. Pitzer, "Manipulator State Estimation with Low Cost Accelerometers and Gyroscopes". In: ed. Philip Roan, Nikhil Deshpande, *2012 IEEE/RSJ International Conference on Intelligent Robots and Systems*, October 7–12, 2012, 4822–4827. DOI: 10.1109/IROS.2012.6385893.

[5] M. Xu, N. Fan, Z. Wang, "Study on Extended Kalman Filtering for Attitude Estimation of Micro Flight Vehicle". In: *Third International Conference on Measuring Technology and Mechatronics Automation*, vol. 3, 2011, 457–460. DOI: 10.1109/ICMTMA.2011.685.

[6] H. Zhao , Z. Wang, "Motion Measurement Using Inertial Sensors, Ultrasonic Sensors, and Magnetometers With Extended Kalman Filter for Data Fusion", *IEEE Sensors Journal*, vol. 12, no. 5, 2012, 943–953. DOI: 10.1109/JSEN.2011.2166066.

[7] Ł. Frącczak, L. Podsędkowski, A. Kobierska, "Data fusion using Fuzzy Logic techniques supported by Modified Weighting factors (FLMW)", *International Journal of Fuzzy Systems*, vol. 18, no. 1, 2016, 72-80. DOI: 10.1007/s40815-015-0095-3.

[8] L. Podsędkowski, H. Podsędkowska „The adaptive optimal Finite Impulse Response smoothing for off - line estimation of the states of the system described by discrete state space model using Extended Output Vector", *Methods and Models in Automation and Robotics MMAR 2015*, 1179–1184. DOI: 10.1109/MMAR.2015.7283984.

[9] P. Żak, "Using 9-axis Sensor for Precise Cardiosurgical Robot Master Angular Position Determination", *Solid State Phenomena*, vol. 199, 2013, 356–361.